A R C H I V E S O F M E T A L L U R G Y A N D M A T E R I A L S
Volume 59 2014 Issue 4
DOI: 10.2478/amm-2014-0282

A.N. WIECZOREK*

THE ROLE OF OPERATIONAL FACTORS IN SHAPING OF WEAR PROPERTIES OF ALLOYED AUSTEMPERED DUCTILE IRON PART II. AN ASSESSMENT OF THE CUMULATIVE EFFECT OF ABRASIVES PROCESSES AND THE DYNAMIC ACTIVITY ON THE WEAR PROPERTY OF AUSFERRITIC DUCTILE IRON

ROLA CZYNNIKÓW EKSPLOATACYJNYCH W KSZTAŁTOWANIU WŁAŚCIWOŚCI ZUŻYCIOWYCH STOPOWYCH ŻELIW SFEROIDALNYCH AUSFERRYTYCZNYCH CZĘŚĆ II. OCENA SKUMULOWANEGO DZIAŁANIA ŚCIERNIWA I WYMUSZEŃ DYNAMICZNYCH NA WŁAŚCIWOŚCI ZUŻYCIOWE SFEROIDALNYCH ŻELIW AUSFERRYTYCZNYCH

The study presents results of the second part of wear tests of austempered ductile irons on a specially designed test rig that allows simulating the real operating conditions of chain wheels. The chain wheels subjected to testing were operated in conditions characterized by combined action of loose quartz abrasive and an external dynamic force. The studies involved the determination of the hardness, microstructure and linear wear of the ADIs in question considered as a function of the austempering temperature and the austenite content. Based on the results obtained, the following was observed: a decrease in the wear as a function of the austempering temperature and thus in the content of austenite in ADIs; a slight deformation of graphite after completing the wear test involving external dynamic forces; a negative linear dependence between the linear wear and the impact resistance. It was found that the increased wear of cast irons with a lower content of austenite may be caused by the propagation of cracks initiated by damage to graphite nodules, while in the conditions characterized by combined action of abrasive wear and dynamic load the cast irons with a higher content of austenite and higher impact resistance have better wear properties.

Keywords: tribology, austempered ductile iron, wear resistance

W pracy przedstawiono rezultaty drugiej części badań zużyciowych stopowych żeliw ausferytycznych na specjalnie skonstruowanym stanowisku badawczym imitującym rzeczywiste warunki eksploatacyjne kół łańcuchowych. Testowane koła łańcuchowe były eksploatowane w warunkach skojarzonego oddziaływania luźnego ścierniwa kwarcowego i zewnętrznej siły dynamicznej. W ramach badań wyznaczono przebiegi twardości, mikrostrukturę i zużycie liniowe rozpatrywanych żeliw ADI w funkcji temperatury ausferytyzacji i zawartości austenitu. Na podstawie uzyskanych wyników zauważono: spadek zużycia w funkcji temperatury ausferytyzacji, a tym samym zawartości austenitu w żeliwach ADI, nieznaczne odkształcenia grafitu po zakończeniu testu zużyciowego z udziałem zewnętrznych sił dynamicznych, zużycie liniowe i udarność wykazały ujemną liniową zależność. Stwierdzono, że powodem zwiększenia zużycia żeliw o mniejszej zawartości austenitu mogła być propagacja pęknięć zainicjowanych uszkodzeniami kulek grafitu oraz w warunkach skojarzonego działania zużycia ściernego i obciążenia dynamicznego lepszymi właściwościami zużyciowymi odznaczają się żeliwa o większej zawartości austenitu charakteryzujące się większą udarnością.

1. Introduction

Simultaneous action of two or more factors accelerating destructive processes occurs often in practical applications. Such a situation may lead to the synergism between processes and the cumulative effect may be much greater than the impact of each process individually. Combined action of destructive factors takes place for example in elements of mining machines. In the case of such machines, the mating elements are subject to abrasive wear, but they are simultaneously exposed to dynamic action of the aggregate and the electrochemical corrosion. Figure 1 shows a sample view of a damaged chain wheel operated in the conditions of combined action of destructive processes, i.e. abrasive wear, corrosion and dynamic load. The factors behind these processes included the abrasive formed as a result of quarrying, water flowing from rock mass as well as falling rock fragments.

In order to ensure the continuity of the operation of machines in harsh conditions, materials and technologies ensuring their failure-free functioning are searched for. Austempered ductile irons (ADIs) constitute one of the groups of materials characterized by good functional properties, including very high wear resistance [1,2,3,4]. Despite the fact that there are many scientific papers concerning ADIs, no studies on properties of ADIs subjected to the simultaneous action of multiple destructive processes are available in the literature.

* SILESIAN UNIVERSITY OF TECHNOLOGY, FACULTY OF MINING AND GEOLOGY, 2 AKADEMICKA STR., 44-100 GLIWICE, POLAND

Fig. 1. A sample view of a damaged chain wheel operated in the conditions of combined action of destructive processes

In the present two-part work investigates the problem of the combined action of abrasive wear intensified by loose quartz abrasive and an external dynamic force. The first part of the study examines the impact of mating of real elements (a chain wheel and a chain) in the presence of quartz abrasive and without it. The chain wheels were made of ADI subjected to isothermal quenching at 4 different temperatures, which resulted in formation of details with different operating properties. Based on the results obtained, the following was found: phase transition of austempered ductile iron can take place for combinations typical of industrial applications, a non-linear increase in the wear as a function of the austempering temperature occurs, an increase in the hardness of all the analysed types of ADI takes place during the operation without the presence of abrasive, the phase transition in ADIs with a lower content of austenite requires higher loads as compared with cast irons containing approx. 40% of austenite.

In the second part of this study, an additional factor was taken into account – the external force of impulse character, which could reduce the service life of the machines by inducing additional stresses in the surface layer.

As already mentioned, the literature of the subject does not include studies on the combined effect of dynamic forces and an abrasive on wear properties of cast irons with an ausferritic structure. However, there are many studies that treat each destructive process separately. The current state of knowledge in the area of abrasive wear resistance is presented in the first part of this paper, while a review of the literature concerning the impact of deformation and dynamic properties of austempered ductile irons is given below.

The impact of dynamic forces on properties of ADI was investigated by Myszka et al. in [5]. Experimental studies with the use of the Taylor test were carried out on samples made of austempered ductile iron and S215 steel. They revealed a high degree of strengthening of both ferrous alloys and an increase in the hardness in the area of dynamic deformation of samples. However, the increase in the hardness of the steel samples was significantly lower than in the case of the cast iron samples. Based on the result of magnetic tests, it was found that martensite occurred in the cast iron matrix as a result of deformation and is a product of the paramagnetic austenite transformation.

Chinella et al. [6] investigated the resistance of ADIs and steel to penetration and damage from a hit by a ballistic projectile. The resistance of these materials varied depending on the type of the projectile used. The ADI with lower hardness and strength was characterised by a better resistance to dynamic action than the ADI with higher hardness and strength. This fact was explained by strengthening of the material under the pressure. A deformation of graphite nodules was also found after the ballistic test.

Olson et al. [7] observed an improvement in mechanical properties, especially in tensile strength and elongation of the ADIs subjected to plastic working immediately after the isothermal quenching.

The impact resistance is a parameter that determines the suitability of individual materials for the operation in dynamic impact conditions. Grech et al. [8] investigated the impact of austempering conditions on dynamic properties of austempered ductile iron with a ferritic structure. The results showed that the austempering parameters, such as temperature and time, affect significantly the impact resistance of the alloy. Eric et al. [9] and Milosan [10] proved, independently of each other, that the impact resistance of ADIs depends on the austempering temperature and time. In general, they found that the impact resistance of alloys grows along with an increase of the austempering time and temperature. The tested parameters were within a processing window that ensured obtaining an ausferritic structure.

The impact of the austenite content, which depends on the process parameters used during austempering, was studied by Grech et al. [11,12] and Dorazil [13]. They proved that the impact resistance of alloys increases along with the percentage content of retained austenite and depends on its stability. Toktas et al. [14] presented results of research examining the effect of the type of ductile iron matrix on the impact resistance of unnotched specimens. There were investigated matrices with a ferritic, pearlitic and martensitic structure as well as with upper and lower ausferritic structure. The highest impact resistance of the ferritic matrix was proved, but the best combination of strength and dynamic parameters was observed in the case of the ausferritic structure. The connection between the impact resistance, austempering conditions, austenite content, and the type of the ausferritic structure was also confirmed in [15,16,17,18,19].

The authors dealing with the problems associated with the wear of ADIs and the dynamic impacts on functional properties emphasise unanimously the importance of phase transitions resulting from mechanical loads. The problem of the phase transition associated with mechanical factors was discussed synthetically in [20]. An ausferritic matrix is formed for certain process parameters associated with isothermal heat treatment of ductile iron. It consists of two types of austenite: the thermally and mechanically stable austenite and the mechanically unstable austenite. Mechanical stability of austenite is associated to a significant degree with the carbon content.

Mechanical instability of austenite at the ambient temperature is similar to the characteristics of austenite in TRIP (TRansformation Induced Plasticity) steel. TRIP is a transformation induced by stress or deformation. Deformation-induced transformation of austenite into martensite (TRIP) is well known and documented for steel [21, 22]. Under this

transformation, the austenite that fulfils specific conditions and is subjected to deformation transforms into martensite (deformation-induced martensite).

This transformation can be explained by thermodynamic processes associated with the martensitic transformation. The transformation is diffusionless and both the austenite and the martensite formed from it have identical chemical compositions. However, each of these phases has a different free energy – respectively $G^{\alpha'}$ and G^{γ}, which will vary along with the temperature (Fig. 2). The state of equilibrium of these phases ($G^{\alpha'} = G^{\gamma}$) will be achieved at the temperature T_0, below which a free energy difference ΔG will appear. This difference will grow along with the increase of supercooling that will reach the temperature M_S at a certain moment. At this temperature, an excess of free energy ΔG will initiate the martensitic transformation.

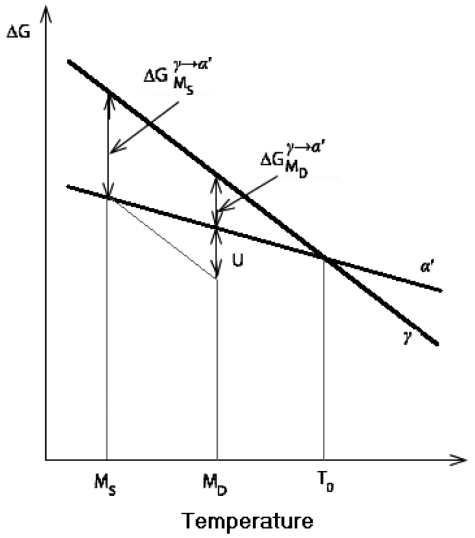

Fig. 2. The dependence between the temperature of the thermal and deformation-induced transformation of austenite and martensite, the free energy AG and the mechanical energy U (based on [20])

However it was documented that an increase of the mechanical energy may result in a decrease/increase of the temperature M_S, depending on whether this energy supports or inhibits this transformation [22]. The martensitic transformation starts when the following dependence is satisfied:

$$\Delta G_{Ms}^{\gamma\rightarrow\alpha'} = \Delta G_{MD}^{\gamma\rightarrow\alpha'} + U \tag{1}$$

where:

$\Delta G_{Ms}^{\gamma\rightarrow\alpha'}$ – free energy of the $\gamma \rightarrow \alpha$' transformation at the temperature M_s,

$\Delta G_{MD}^{\gamma\rightarrow\alpha'}$ – free energy of the $\gamma \rightarrow \alpha$' transformation at the temperature M_D,

U – mechanical energy.

The temperature, at which the martensitic transformation supported by mechanical energy starts, is designated as M_D (Fig. 2). It was found that the transformation will not occur above this temperature, even if the maximum amount of free energy is supplied to the system [22]. Mechanically unstable austenite may occur in any type of austempered ductile iron. It is characterized by a susceptibility to static and dynamic impacts if the stresses induced in the material have a sufficiently high value. It was found that the occurrence of a deformation-induced transformation can be identified almost in every process associated with exceeding the yield point and with the deformation of ausferrite. The issue of the transition of austenite into martensite in austempered ductile irons has been described also in [23,24,25,26].

2. Experimental details

Experimental studies were conducted on the test rig described in detail in the first part of this paper. The combined effect of the abrasive wear caused by loose quartz abrasive and the action of an external force was reproduced by filling the test box with quartz abrasive and adding steel beaters hitting the chain wheel during the wear tests. In relation to the abrasive wear in the presence of an external dynamic force, the term "abrasive-dynamic wear" was used in this paper.

A diagram of the load generated by the force resulting from the driving torque and an external dynamic force is shown in Fig. 3. Figure 4 presents a view of the test rig during the wear tests, as well as the manner of mounting the beaters.

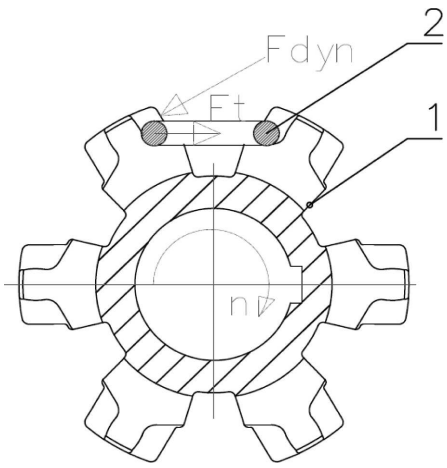

Fig. 3. Load diagram of the sample (chain wheel); designations: 1 – chain wheel, 2 – chain, Ft – driving force, Fdyn – additional dynamic force

A set of chain wheels designated as ADI_240_D, ADI_270_D, ADI_310_D and ADI_360_D was used for the wear tests. The main wear tests were carried out in the presence of loose quartz abrasive. They lasted for 200 hours in total: 100 hours for the counter-clockwise direction of both motors and 100 hours for the clockwise direction. The research methodology, the selection of materials for testing and the method of determining the wear parameters were the same as in the first part of this study.

Introduction of an additional dynamic load in the form of beaters did not change significantly the stress values occurring during the operation of the chain wheel in the area of mating with the chain as compared with the operation of chain wheels in conditions of abrasive wear alone. This finding was made on the basis of a simulation with the use of the FEM method.

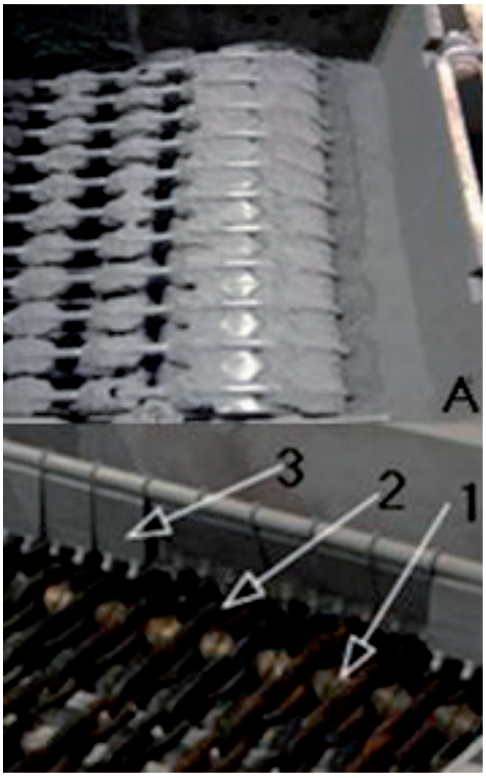

Fig. 4. Test rig A. View of the box of the test rig during the tests; B. Vew of the test rig with the following elements installed: chain wheels (1), chains (2) and beaters (3), which induce the dynamic load

3. Result and discussion

As in case of the wear tests of chain wheels made of ADI carried out only in the presence of quartz abrasive, an observation was made that the abrasive was crushed between mating surfaces of the teeth and the chain. After approx. 10 hours of operation, crushing of the abrasive significantly decreased and the size of quartz grains was less than 20 μm.

The leading destructive process was microcutting (presented better in Fig. 12), by loose quartz abrasive with hardness higher than that of wheel surface. Figure 5 shows clear abrasions in mating surfaces of the tooth and the chain caused by abrasive wear. The abrasions were smooth and shiny, while small cavities could be seen in some mating areas. There are neither signs of adhesive damage nor an impact of thermal overheating caused by friction.

After removing the shafts with the wheels subjected to testing, measurements were performed using the coordinate measuring machine in order to determine the value of the linear wear (Table 1).

TABLE 1
The determined parameters characterizing the dynamic and abrasive wear

Designation of sample	δ_{AVR_MAX}, *mm*	S_δ, *mm*	$S_{\delta x}$, *mm*
ADI_360_D	0.78±0.09	0.22	0.045
ADI_310_D	0.89±0.11	0.27	0.055
ADI_270_D	0.91±0.12	0.30	0.06
ADI_240_D	0.99±0.13	0.31	0.064

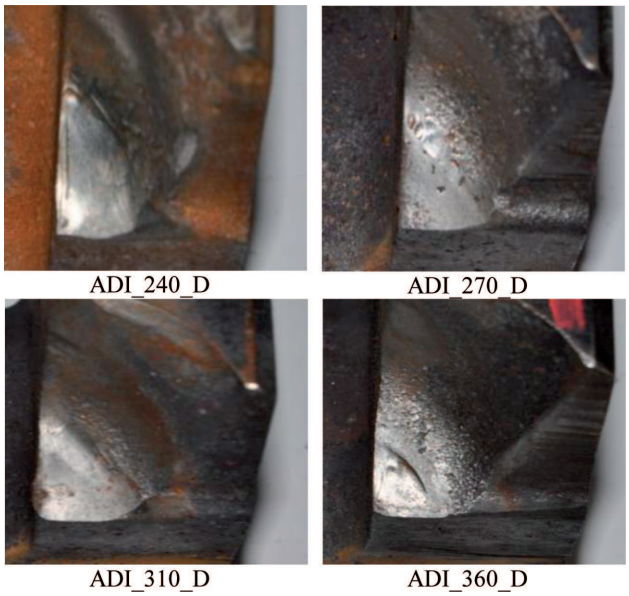

Fig. 5. Traces of local abrasions on surfaces of teeth of the chain wheels tested

Figure 6 shows a plot of the wear values determined as a function of the austempering temperature of ADIs. A decrease in the linear wear along with an increase in the austempering temperature of the cast irons can be observed in this figure. The plot is characterized by a completely different dependence than the one presented in the first part of this paper for chain wheels subjected to the abrasive wear. First of all, a linear dependence between the wear and the austempering temperature can be seen.

After measurements of teeth geometry had been performed, distributions of Vickers hardness HV0,1 (Fig. 7) were determined and Brinell hardness was measured (Table 2). The plots obtained are characterized by considerable variability of the Vickers hardness in the range from 0 to 0.5, however a relatively small difference between the maximum value determined and the core hardness is observed.

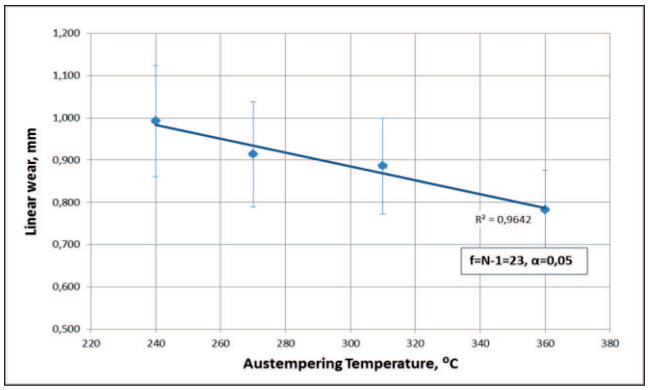

Fig. 6. The wear of test samples as a function of the austempering temperature

After the wear tests, samples for metallographic examinations were cut out from the area of mating between the chain wheel and the chain. Then the samples were ground, polished and etched with a 2% Nital solution. The microstructures obtained are shown in Fig. 8–11.

Figure 8 shows the microstructure of ADI isothermally quenched at the temperature of 240°C (ADI_240_D) after

the tests. Nodular graphite and lower ausferrite (composed of ferrite, austenite and probably small amounts of martensite) can be identified in the structure. In the image of the microstructure obtained at the magnification 200x, oblique cavities caused by the action of wedge-shaped abrasive can be observed. The deformation of the graphite nodules is relatively small. Locations of deeper cavities include generally the areas vacated by graphite nodules.

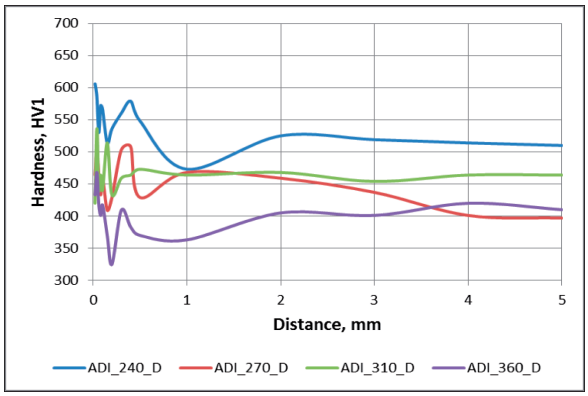

Fig. 7. The Vickers hardness HV0,1 as a function of the distance from the surface of chain wheels (the maximal relative measurement uncertainty was 1% determined for f=N-1=4 and α =0.05)

TABLE 2
Values of the maximum hardness HV_{MAX}, core hardness HV_{CORE} and Brinell surface hardness HB surface obtained for the chain wheels tested in the presence of a quartz abrasive and a dynamic load (the maximal relative measurement uncertainty was 1% determined for f=N-1=4 and α =0.05)

Designation	HV_{MAX}	HV_{CORE}	*HB*
ADI_360_D	606±6	508±5	395±4
ADI_310_D	508±5	432±4	379±4
ADI_270_D	536±5	463±5	342±3
ADI_240_D	468±5	400±4	279±3

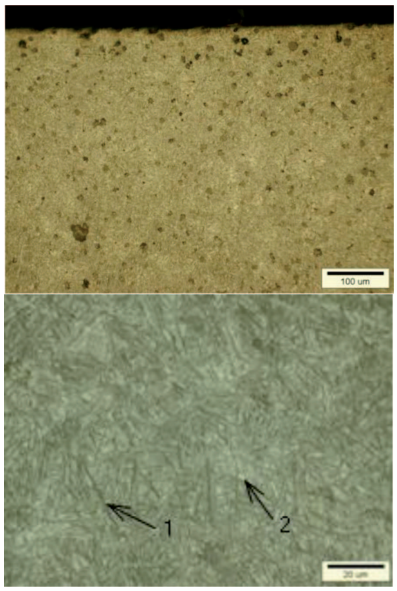

Fig. 8. Microstructure of ADI_240_D (magnification: upper picture – 200x, lower picture – 1000x; 1 – bainitic ferrite, 2 – austenite

The microstructure of the ADI_270_D matrix (Fig. 9) consists of lower ausferrite with the austenite content of approx. 20%. In the image of the microstructure obtained at the magnification 200x, wedge-shaped signs of damage after the destruction of graphite nodules can be seen. In some cases the area between microcuts crumbled away. The spherical shape of graphite nodules in the surface layer was maintained without changes.

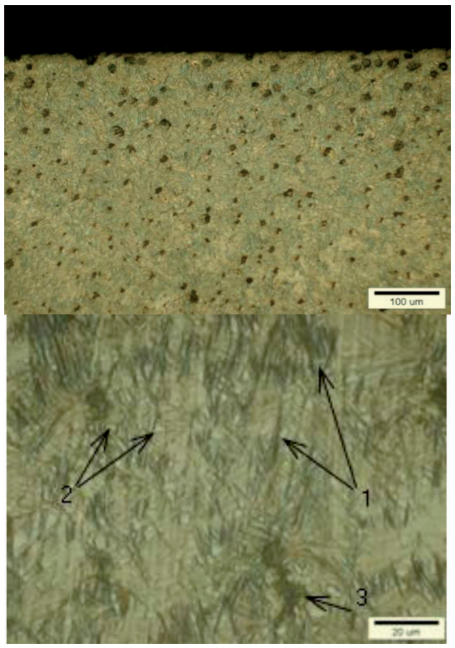

Fig. 9. Microstructure of ADI_270_D (magnification: upper picture – 200x, lower picture – 1000x); 1 – bainitic ferrite, 2 – austenite, 3 – graphite

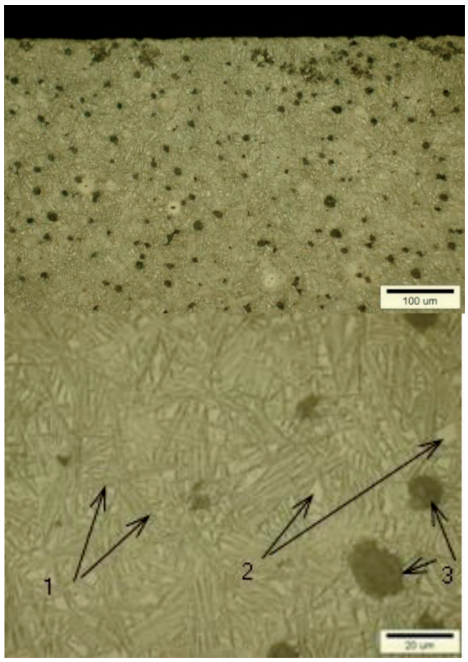

Fig. 10. Microstructure of ADI_310_D (magnification: upper picture – 200x, lower picture – 1000x)); 1 – bainitic ferrite, 2 – austenite, 3 – graphite

As compared with the variants discussed earlier, the ADI_310_D variant (Fig. 10) is characterized by shallower

cavities, without distinct directionality, and clusters of graphite located at the surface. The shape of graphite departs significantly from the spherical shape (presented in Fig. 12), typical for the graphite located at a surface exposed to the action of abrasive [27,28]. The matrix of ADI_310_D consists of upper ausferrite with the austenite content of approx. 27%.

Figure 11 shows the microstructure of the cast iron designated as ADI_360_D. The matrix microstructure is also composed of upper ausferrite, however the content of austenite is approx. 40%. On the surface of the sample there are visible shallow cavities perpendicular to the surface. It is characteristic that ferrite plates in the surface layer (at a depth down to approx. 0.2 mm) are highly fragmented, while ferrite plates below this depth are almost twice bigger.

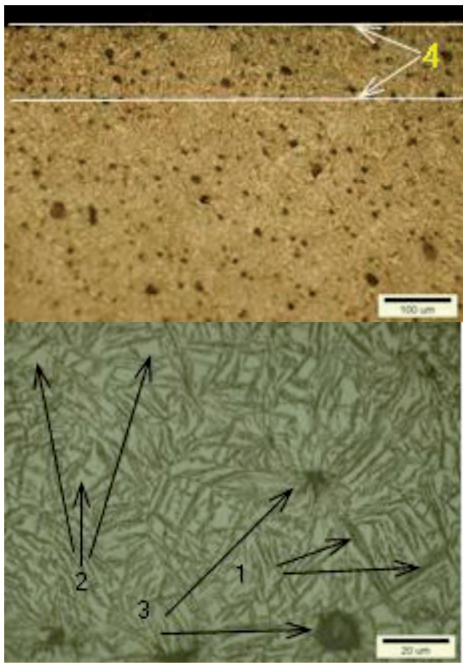

Fig. 11. Microstructure of ADI_360_D (magnification: upper picture – 200x, lower picture – 1000x)); 1 – bainitic ferrite, 2 – austenite, 3 – graphite, 4 – zone of particulate ferrite

The fact that there is more damage to the surface as a result of a decrease of the impact resistance suggests a considerable importance of the effect of austenite content on the complex dynamic and abrasive excitations occurring in the test rig. When comparing the results of wear tests for the abrasive variant and the dynamic-abrasive variant (Table 3 and Fig. 13) as a function of the percentage content of austenite, it can be noticed that the plots are quite different. In the case of the abrasive variant, the wear generally increases along with an increase in the austenite content, while for the dynamic-abrasive variant the wear decreases along with an increase in the austenite content. The linear wear values are very similar only for the austenite content equal to 27%.

When expressed in percentage (Table 4), the use of the beaters simulating an external dynamic load caused an increase in the wear by almost 29% for the cast iron with the austenite content of 12%, while for the cast iron containing 27% of austenite the increase was approx. 12%. The wear of cast irons with a higher content of austenite (27% and 40%) decreased by 4 and 19%, respectively.

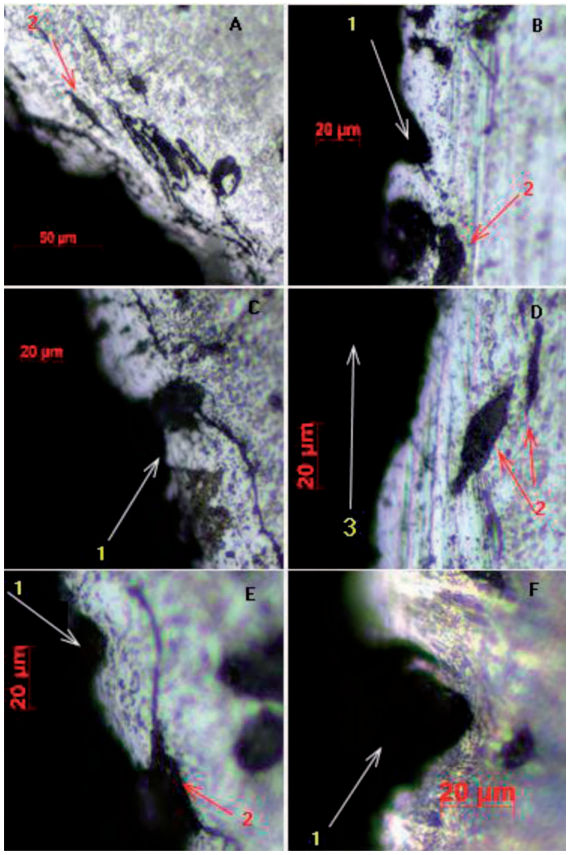

Fig. 12. Microcuts (1) and deformation of graphite nodules (2) in microstructure of ADI_310_D; 3 – Direction of force

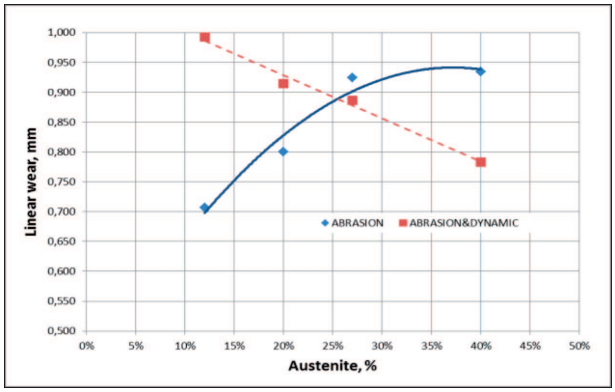

Fig. 13. The wear of test samples as a function of the percentage content of austenite

TABLE 3

Comparison of the linear wear values obtained for the abrasive variant (right part of the table) and for dynamic-abrasive variant (left part of the table)

Designation of sample	δ_{AVR_MAX}, *mm*	*Designation of sample*	δ_{AVR_MAX}, *mm*
ADI_360_D	0,783	*ADI_360*	0,934
ADI_310_D	0,886	*ADI_310*	0,924
ADI_270_D	0,914	*ADI_270,*	0,801
ADI_240_D	0,993	*ADI_240,*	0,707

TABLE 4

Relative difference of the linear wear $\Delta\delta_{AVR}$, %

Designation	$\Delta\delta_{AVR}$, %
(ADI_240_D - ADI_240)/ ADI_240_D	28.78%
(ADI_270_D - ADI_270)/ ADI_270_D	12.42%
(ADI_310_D - ADI_310)/ ADI_310_D	-4.29%
(ADI_360_D - ADI_360)/ ADI_360_D	-19.27%

Figure 14 shows plots of the linear wear δ_{AVR} of the samples tested for the abrasive-dynamic wear variant as well as plots of the impact resistance as a function of the percentage content of austenite. An inversely proportional dependence between the wear and impact resistance values determined was observed. The value of the Pearson's correlation coefficient determined for the linear wear and the impact resistance was r_{xy} = - 0.989, which suggests a negative linear relationship between these features.

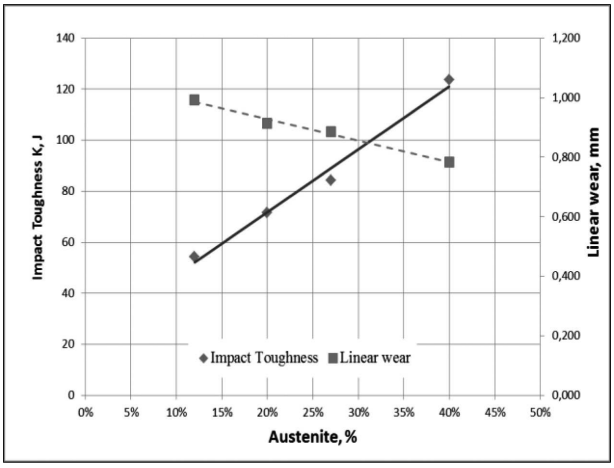

Fig. 14. Linear wear of the test samples for the abrasive-dynamic wear variant and the impact resistance of the samples as a function of the percentage content of austenite

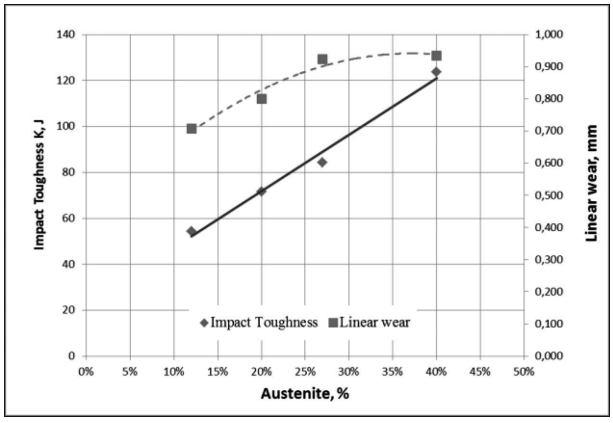

Fig. 15. Linear wear of the test samples for the abrasive wear variant and the impact resistance of the samples as a function of the percentage content of austenite

Figure 15 shows plots of the linear wear δ_{AVR} of the samples tested for the abrasive wear variant as well as plots of the impact resistance as a function of the percentage content of austenite. The value of the Pearson's correlation coefficient determined for this case was r_{xy} = 0.856, which suggests that relationship between the features is not very strong and that in the case of the abrasive wear the impact resistance is not the main feature affecting the wear of cast irons.

In the case of the abrasive wear variant, the main parameter affecting the wear is rather the hardness. This is confirmed by Fig. 16, which shows plots of the linear wear δ_{AVR} of the samples tested for the abrasive wear variant as well as plots of the Brinell hardness HB as a function of the percentage content of austenite. The value of the Pearson's correlation coefficient determined in this case was r_{xy} = - 0.942. A negative linear relationship between the linear wear and Brinell hardness can be seen in this case.

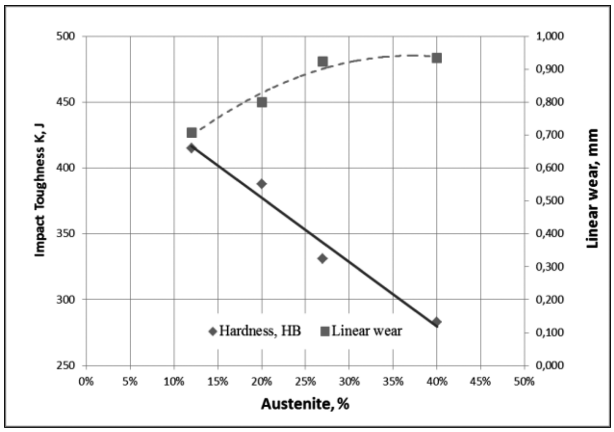

Fig. 16. Linear wear of the test samples for the abrasive wear variant and the HB hardness of the samples as a function of the percentage content of austenite

Figure 17 shows a comparison of plots of Vickers hardness HV0,1 for chain wheels worn in the presence of abrasive, with an external force and without it. It is easy to notice that, except for the case of the cast iron quenched at the temperature of 310°C, higher values of the Vickers hardness occur after the wear in the presence of abrasive without an additional dynamic force than in the case of the abrasive-dynamic wear.

Table 5 summarises the values of the hardness difference for the abrasive wear variant and the abrasive-dynamic variant (ΔHV_{MAX} and ΔHB). The hardness differences ΔHV_{MAX} and ΔHB increase along with a reduction of the austenite content in the cast irons tested.

The results of tests concerning the linear wear and the hardness of ADI surfaces indicated an important role of operational factors (e.g. loads and the presence of abrasive) in shaping of wear properties, which to a significant degree depend on phase transitions.

The impact of operational factors (i.e. the abrasive and the dynamic loads) caused a change in the character of the plots of the hardness and wear as a function of the austenite content. The vibrations of the chain occurring in the area of mating between the wheel and the chain, induced by the impulse of the force F_{dyn} opposite to the force F_t, could impact on the martensitic transformation and microstructure of ADI (for example, on the Fig. 11 can see fragmentation of ferrite plates in the surface layer). A reduction in the hardness of the surface layer for the abrasive-dynamic wear variant suggests a lower intensity of the transformation of austenite into martensite.

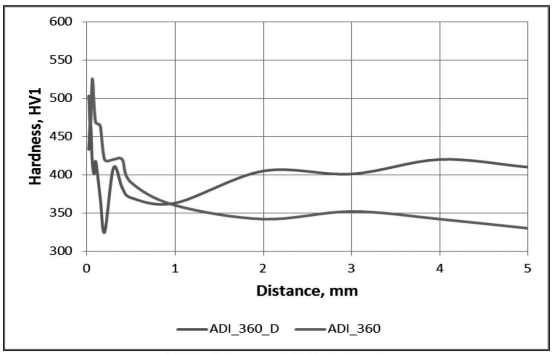

ADI_360 vs. ADI_360_D

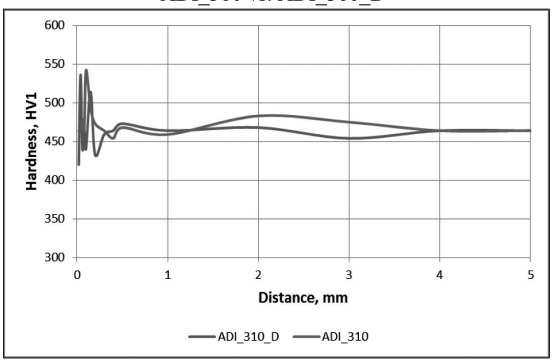

ADI_310 vs. ADI_310_D

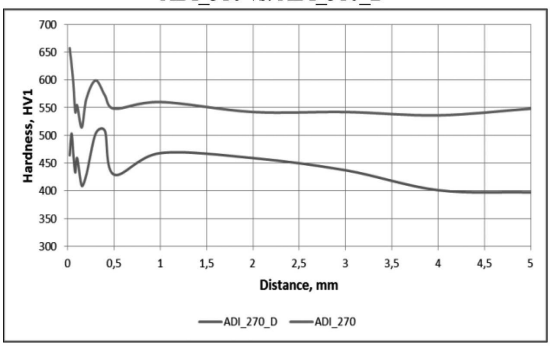

ADI_270 vs. ADI_270_D

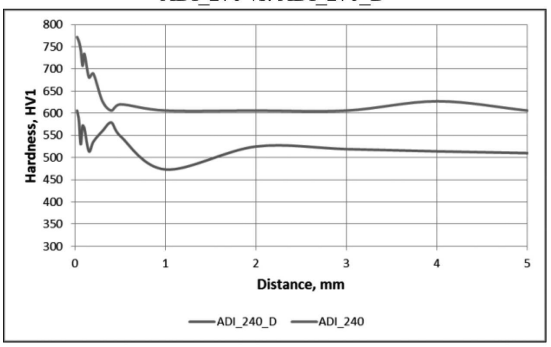

ADI_240 vs. ADI_240_D

Fig. 17. A comparison of plots of Vickers hardness HV0,1 for chain wheels worn in the presence of abrasive, with an external force and without it

However, the decrease in the intensity of phase transitions in the matrix was not the main reason for an increased wear of cast irons with a lower content of austenite (ADI_240_D and ADI_270_D). Lower ausferrite is characterized by a better wear resistance [29] and a greater strength [32] than the upper ausferrite.

Causes of an increased wear of cast irons with a lower content of austenite should be sought in graphite. During the wear tests, it happened that beaters hit the tip of the tooth of the chain wheel tested. The number of hits was significant, i.e. approx. $3.6 \cdot 10^5$. As already mentioned, the hits did not cause any increase of stresses at the contact with the chain, but they could generate microcracks on the surface and damage graphite nodules. The graphite occurring in the ADI structure is susceptible to mechanical damage, thus hits of the beaters could lead to fracture of graphite nodules.

TABLE 5
Values of the hardness difference for the abrasive wear variant and the abrasive-dynamic variant (ΔHV_{MAX} and ΔHB)

Designation	ΔHV_{MAX}	ΔHB
ADI_240 - ADI_240_D	166	97.8
ADI_270 - ADI_270_D	149	103.6
ADI_310 - ADI_310_D	6	-37.8
ADI_360 - ADI_360_D	57	9.2

Sharma [30] and Vrbka et al. [31] found a 60 – 82% decrease in the resistance to fatigue pitting in lubricated austempered irons subjected to shot peening as compared with surfaces not subjected to shot peening. Shot peening is a dynamic treatment affecting the stress conditions in the surface layer. In the case of ADIs it initiates phase transformations of austenite into martensite. However, shoot peening causes damage to graphite and even its complete destruction. The resulting cracks and the voids formed after the removal of graphite contributed to propagation of damages into the matrix of ADIs.

Chawla et al. [32] examined properties of the microstructure of ADIs subjected to the action of dynamic forces. They found that a crack always started at the contact of graphite nodules and the matrix, while it was generally propagated along the austenite and ferrite plates. The authors also noted that the direction of crack propagation depended on the direction of the load applied.

In the case considered in this study, cracks initiated at the contact between graphite and the matrix could facilitate the propagation of cracks deep into the material, which could in turn facilitate microcutting of the surface layer of the chain wheels by crushed abrasive. A relationship between the wear and the impact resistance was found under this study. A lower impact resistance, despite a higher strength of lower ausferrite, could be the reason for an easier propagation of cracks in conditions of the impact of the dynamic load induced by beaters. In the case of ADIs with a higher content of austenite (ADI_360_D and ADI_310_D), which are characterized by a higher impact resistance, a fewer number of cracks in the matrix and even in the graphite could be observed due to their better plastic properties.

4. Conclusions

1. Based on the tests of chain wheels performed in controlled conditions of abrasive wear with the participation of external dynamic forces, there was found a decrease of the wear as a function of the austempering temperature, and thus a decrease in the content of austenite in ADIs.

2. Slight deformations of graphite after completing the wear test with the participation of external dynamic forces were identified.
3. An observation was made that in the case of abrasive wear with the participation of external dynamic forces, there occurred a negative linear dependence between the linear wear and the impact resistance.
4. In the conditions of the combined effect of the abrasive wear and the dynamic load, cast irons with an increased content of austenite have better wear properties and are characterised by a higher impact resistance.

Acknowledgements

The study was carried out as a part of the project "Innovative technology for production of tension members for transport systems with the use of cast materials", No. POIG.01.04.00-24-100/11.

REFERENCES

[1] K.L. Hayrynen, J.R. Keough, AFS Transactions **187**, 1-10 (2005).
[2] K.L. Hayrynen, J.R. Keough, G.L. Pioszak, AFS Transactions, 1-15 (2010).
[3] E. Guzik, Archiwum Odlewnictwa. Monografia 1M, 1-128 (2001).
[4] E. Guzik, Archives of Foundry **6/21**, 1-2 (2006).
[5] D. Myszka, T. Cybula, A. Wieczorek, Archives of Metallurgy and Materials **59**, 1181-1189 (2014).
[6] J.F. Chinella, B. Pothier, M.G.H. Wells, Processing, Mechanical Properties, and Ballistic Impact Effects of Austempered Ductile Iron. Army Research Labaratory, ARL-TR-1741 August 1998.
[7] B.N. Olson, D.J. Moore, K.B. Rundmam, G.R. Simula, AFS Transactions **111**, 965-982 (2002).
[8] M. Delia, M. Alaalam, M. Grech, Journal of Materials Engineering and Performance **7(2)**, 265-272, (1998).
[9] O. Erić, M. Jovanović, L. Šidanin, D. Rajnović, S. Zec, Materials and Design **27**, 617-622, (2006).
[10] I. Milosan, European Scientific Journal **3** 149-153 (2013).
[11] M. Grech, J.M. Young, Cast Metals **8**, 98-103 (1987).
[12] M. Grech, P. Bowen, J.M. Young, 3rd World Conference on ADI, Chicago, 338-374 (1991).
[13] E. Dorazil, Foundry **160**, 36-45 (1986).
[14] G. Toktaş, M. Tayanç, A. Toktaş, Materials Characterization **57**, 290-299 (2006).
[15] M.R. Jahangiri, M. Ahmadabadi Nili, H. Farhangi, Journal of Materials Engineering and Performance **20/9**, 1642-1647 (2011).
[16] B. Uma, R. Subrata, S.R. Prabhakar, JMEPEG **16**, 485-489 (2007).
[17] E. Dorazil, High Strength Austemperd Ductile Cast Iron, Horwood Series in Metals and Associated Materials (1991).
[18] R.A. Harding, Kovove Mater. **45(1)**, 1-16 (2007).
[19] A. Polishetty, S. Singamneni, G. Littlefair, ASME 2008 International Manufacturing Science and Engineering Conference **1**, 49-57 (2008).
[20] D. Myszka, Monografia, Prace Naukowe Politechniki Warszawskiej, z. 265 Inżynieria Produkcji (2014).
[21] H.K.D.H. Bhadeshia, Bainite in Steels, The Institute of Materials, Cambridge (2001).
[22] J. Jeleńkowski, Oficyna Wydawnicza Politechniki Warszawskiej, (2005).
[23] J. Aranzabal, I. Gutierrez, J.M. Rodriguez-Ibabe, J.J. Urcola, Metalluragical and materials transactions **28a**, 1143-1156 (1997).
[24] A.S.M.A. Haseeb, M. Aminul Islam, Wear **244**, 15-19 (2000).
[25] J.L. Garin, R.L. Mannheim, Journal of Materials Processing Technology **143-144**, 347-351 (2003).
[26] D. Myszka, E. Skołek, A. Wieczorek, Archives of Metallurgy and Materials **59/3**, 1227-1231 (2014).
[27] D. Myszka, A. Wieczorek, Material Engineering (Inżynieria Materiałowa) **4/194**, 332-335 (2013.
[28] D. Myszka, A. Wieczorek, Archives of Metallurgy and Materials **58/3**, 967-970 (2013).
[29] J. Kaleicheva, Tribology in Industry **36/1**, 74-78 (2014).
[30] V.K. Sharma, Journal of Heat Treating **3**, 326-334 (1984).
[31] M. Vrbka, I. Křupka, P. Svoboda, P. Šperka, T. Návrat, M. Hartl, and J. Nohava, Tribology International **44**, 1726-1735 (2011).
[32] V. Chawla, U. Batra, D. Puri, A. Chawla, Journal of Minerals & Materials Characterization & Engineering **7**, 4, 307-316 (2008).

Received: 20 October 2013.